LA-UR- 98-2671

Engineering Development of Superconducting RF Linac for High-Power Applications

K. C. Dominic Chan, Brian Rusnak, Robert C. Gentzlinger, Billy M. Campbell, J. Patrick Kelley,
Los Alamos National Laboratory, Los Alamos, NM 87544, USA
Henri Safa, CEA Saclay, France

Abstract

High-power proton linacs are a promising source of neutrons for material processing and research applications. Superconducting radiofrequency (SCRF) RF linac technology is preferred for such applications because of power efficiency. A multi-year engineering development program is underway at Los Alamos National Laboratory to demonstrate the required SCRF technology. The program consists of development of SC cavities, power couplers, and cryomodule integration. Prototypes will be built and operated to obtain performance and integration information, and for design improvement. This paper describes the scope and present status of the development program.

1 INTRODUCTION

High-power proton linacs have been proposed as drivers of neutron sources [1]. These linacs nominally have energies of 1-GeV and CW currents of 100 mA. At this high beam power, they are required to be electrically efficient and have low beam loss. These requirements can be readily satisfied with an SCRF linac that has negligible structure RF losses and a large beam aperture [2].

To apply SCRF technology for high-power proton linacs, we need to extend the technology to accelerate non-relativistic ($\beta<1$) beams and to high beam power. A multi-year program is now underway at for such a technology demonstration [3]. The program will develop SCRF components, including elliptical cavities for $\beta<1$ beam, and power couplers for transmitting high (210 kW) RF powers. It will integrate these components to build prototype cryomodules for a proposed SCRF linac, as shown in Figure 1. Because of the large velocity acceptance of short SCRF cavities, the SCRF linac is composed of cryomodules with only two β designs (β=0.64 and 0.82 respectively). Present efforts are primarily directed towards the β=0.64 design.

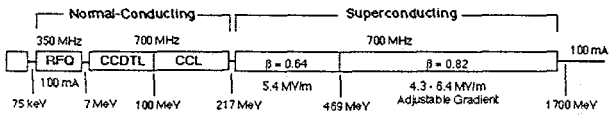

Figure 1: Layout of a proposed high-power proton linac.

2 ELLIPTICAL NIOBIUM CAVITIES

The SC cavities are 5-cell cavities fabricated with Niobium sheets. The cells have elliptical shapes typical of SC cavities except that the accelerating gaps are reduced to match the lower β. The required field gradient (Ea) varies between 4.3 to 6.5 MV/m along the linac. This required performance is conservative compared to the achieved Ea recently reported by other laboratories [4] and will keep the peak surface field to below 16 MV/m.Recently, we have completed a series of single-cell cavity measurements at an operating temperature of 2 K. Results [5] showed that this field performance can be achieved with Q_o better than 5×10^9, with readily available niobium material (RRR=250) and a processing technique without cavity heat treatment. There is more than a factor of two margin in the achievable fields. Results also showed that the required fields were achieved with no multipacting, although the $\beta<1$ cells have relatively parallel side walls.

2.1 Design

Figure 2 shows the β=0.64 cavity design. The niobium thickness (4-mm) and the sidewall slope (10-degree) were chosen to withstand vacuum load and cooldown pressure excursions without any mechanical stiffeners, to reduce cost.

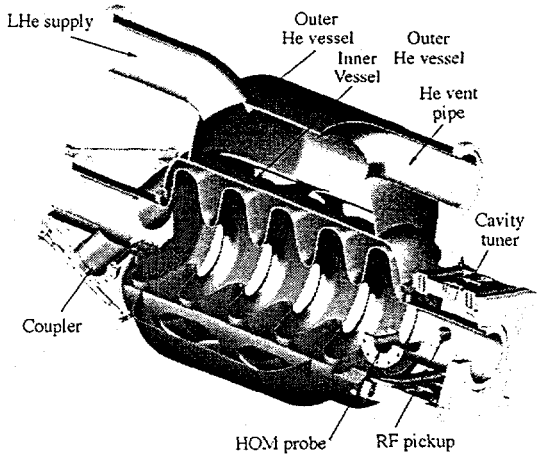

Figure 2: Design of 5-cell cavity with helium vessel and tuner.

The beam pipes at the cavity ends have an aperture radius of 6.5 cm. This aperture size is increased to 8.0 cm between the coupler and the cavity, to obtain a high coupler coupling coefficient with the cavity. The cavity assembly has a total length of 1.16-m (active length of 0.69 m). The cell radius is 21 cm.

DISCLAIMER

The cavity is contained in a cylindrical inner helium vessel and a cylindrical outer helium vessel. This design provides the required mechanical strength and the volume for helium expansion during cryogenic operational transients. The vessels are made of titanium, which has a thermal expansion coefficient similar to that of niobium, to reduce mechanical stresses due to differential thermal expansion.

The tuner is designed similarly to those used satisfactorily at CESR. It has a tuning range of ±324 kHz. All its drive mechanisms are installed outside the cryostat for operation at ambient temperature and pressure, allowing easy maintenance and reducing the chance of failure at cryogenic temperature

2. 2 Status

We have completed our single-cell cavity measurements for β=0.48 and 0.64 cavities. We finished the engineering design of β=0.64 5-cell cavities and have awarded a contract to fabricate four such cavities. In addition, we are also fabricating one such cavity at Los Alamos for testing in July 1998.

3 COAXIAL COUPLERS

Because of the high current, we need to supply 420 kW to each cavity for beam acceleration. This power is supplied with two power couplers, each carrying 210 kW. Presently, the highest power transmitted by any coupler with beam operation is below 180 kW. The required power level for our couplers is a reasonable extension of existing technology. We have chosen the coaxial-type coupler because of its demonstrated power-handling capability and ongoing work in other laboratories[6]. At this power level, we need to pay special attention to minimizing RF reflection and RF losses as a thermal load to the cryogenic system.

3.1 Design

Figure 3 shows the power coupler design. The coupler consists of three assemblies: the window assembly, the coaxial coupler, and the transition.

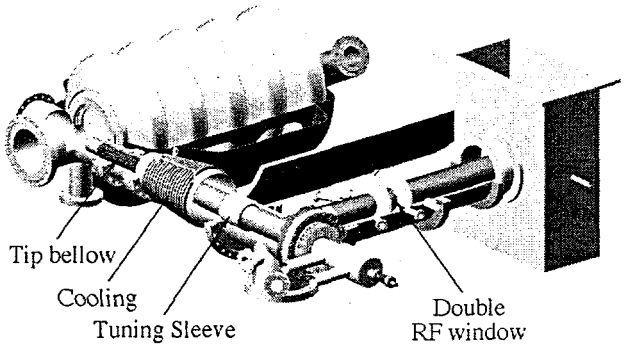

Coaxial coupler Transition Window assembly

Figure 3: Design of the power coupler.

Because RF windows are usually the primary source of failures for couplers, we have chosen to use warm RF windows that do not have direct line-of-sight to the beam. The window assemblies are manufactured as an integrated unit by klystron manufactures that have experiences in building warm RF windows with high reliability. For enhanced lifetime, these window assemblies are designed for 1-MW CW power operation and are equipped with diagnostics to detect signs of failure onset. Each assembly has two ceramic windows with a limited supply of cooling gas between them, so we can keep the linac operating in the event of a window failure. Replacement of the failed window can then be delayed until scheduled maintenance periods.

The coaxial coupler assembly has a characteristic impedance of 50 ohms. The outer conductor has a tapered section from a 6-1/8 inches diameter to 4-inches. It is made of copper plated (15 μm thick plating) stainless steel. The inner conductor is made of copper. The inner conductor has a BeCu formed bellows to allow for a factor of three coupling-coefficient adjustments.

The transition assembly provides the RF matching between the window and coaxial coupler assemblies. It performs the matching with a quarterwave short and a tuning sleeve. The shapes of these components are optimized with extensive 3-D electromagnetic simulations using the MAFIA code. Extensive simulations of individual assembly and the complete coupler have been done to minimize RF reflection and interactions between assemblies. They are also used to ensure there are no field enhancements that will lead to local overheating or multipacting.

The coupler is a major thermal path between room temperature and 2 K. Because of RF losses, it is also an important heat source. For optimized thermal management, a thermal model has been constructed to evaluate different cooling schemes by their impacts to the wall power required to handle the resulting refrigeration loads. In the present design, the center conductor is cooled by forced convection with gaseous helium at 300 K, although there is a strong possibility that this temperature will be reduced. We are in the process of choosing a cooling scheme for the outer conductor. The most likely candidates are a two-point thermal intercept and a counter-flow heat-exchanger intercept.

3.2 Status

A review of the electromagnetic, mechanical, and thermal design of the coupler occurred in April 1998. Currently, couplers are being fabricated for tests. Double RF windows have been ordered and will be tested in August 1998. We are evaluating different copper plating processes with respect to mechanical properties, vacuum properties, and RF resistivities of the plating.

4 CRYOMODULE

The cryostat design is based on the LEP-II cryomodule design [7] that has removable vacuum-vessel panels for easy access.

4.1 Design

Figure 4 shows the cryomodule design. The cryostat is made from 310 stainless steel. It consists of three sections: two end sections and a center section. For the β=0.64 design, the center section houses two helium vessels of the cavities. The center section will go into the cleanroom so that cavities and power couplers can be installed. Like the LEP-II design, the center section has large top and bottom openings. These openings, which permit easy access and allow for laminar air flow during cleanroom assembly, are closed with recessed structural panels and covered with a skin that seals on an o-ring to form the vacuum seal. The helium vessels of the cavities are supported with spokes that attach to the cryostat. A flexure attached to each power coupler outside the cryostat will constrain the coupler in five degrees of freedom. The radial direction is left free to permit contraction during cool down. The thermal shield is made of an aluminum cylinder that is assembled from upper and lower halves. Each half is cooled with a single aluminum tube attached by welding to tabs on the thermal shield. There will be blankets of multilayer insulation made of aluminized mylar, placed on the thermal shield and on the helium vessels. A passive magnetic shield is made up of two layers of cryoperm and will reduce the magnetic field at the cavities to 10 mGauss. We are also assessing the use of Helmholtz coils for attenuating the axial magnetic shield. The cavities and power couplers share a common ultra-clean turbopumped vacuum system. The pumping is provided by turbopumps. A separate turbopumped system is used for the insulating vacuum during initial pump down of the cryostat. After cool down, most of the pumping will be provided by the cool surface of the helium vessel, supplemented by a small turbopump.

The cryomodule is supplied with supercritical helium at 2.6 K and 3 ATM. After entering the cryostat, it will expand through a Joule-Thompson valve to 0.046 ATM, forming the 2-phase He II that is then phase separated. The liquid helium is transported to the first cavity through a 15-cm duct connecting the helium vessels. Helium vapor is transported back to the refrigeration plant through a similar sized duct that connects the helium vessels and the top of the downstream helium vessel. Liquid helium is provided to the downstream cavity through a 2-cm line that connects the bottoms of the two helium vessels. This line also allows for equilibration of liquid levels in each vessel.

4.1 Status

A conceptual design review was held September, 1997. Since then, we have been improving and modifying the conceptual design. A final design review is scheduled for September, 1998.

5 CONCLUSION

A program to develop SCRF technology for high-power linac applications is now well underway at Los Alamos. We will be testing cavities and power couplers in the next six months.

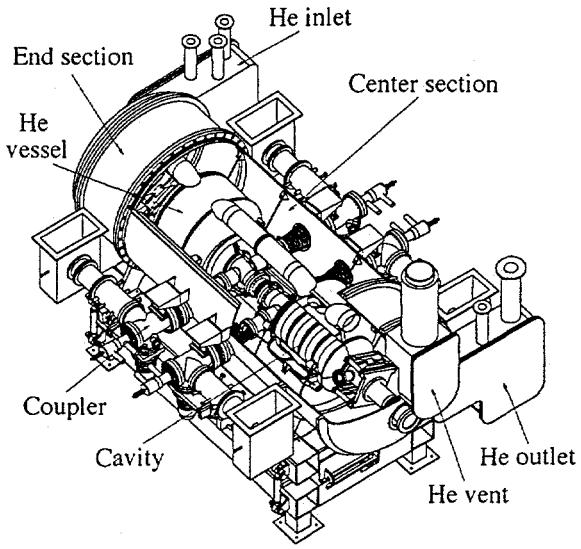

Figure 4: Cryomodule design.

REFERENCE

[1] C.D.Browman et al., "Nuclear Energy Generation and Waste Transmutation Using Accelerator-driven Intense Neutron Source," Nucl. Instr. And Meth. A320(1/2) (1992) 336-367.

[2] K.C.D.Chan, "Conceptual Design of a Superconducting High-Intensity Proton Linac," Proc. of the XVIII Int. Linac Accel. Conf, 26-30 August 1996, Geneva, Switzerland, pp. 580-582.

[3] K.C.Chan et al., "Development of RF Linac for High-current Application," to be published in Nulc. Instr. and Meth.

[4] D. Proch, et al., presented at the 1997 Part. Accel. Conf., May 12-16, Vancouver, B.C. Canada.

[5] W.B.Haynes et al., "Medium-Beta Superconducting Cavity Tests at Los Alamos National Lab for High-Current Proton Linac," presented to the 8th Workshop on RF Superconductivity, Oct. 6-11, 199?, Padova, Italy.

[6] Akai, et al., presented at the 1997 Part. Accel. Conf., May 12-16, Vancouver, B.C. Canada.

[7] G.Cavallari et. al., Proceedings of the 5th Workshop on Rf Superconductivity, Hamburg (1991).